

# Low-Cost Turbidity Sensor for Low-Power Wireless Monitoring of Fresh-Water Courses

Youchao Wang, S. M. Shariar Morshed Rajib, Chris Collins, and Bruce Grieve

**Abstract**—This paper reports on a low-cost turbidity sensor design for continuous on-line water quality monitoring applications. The measurement of turbidity by agricultural and environmental scientists is restricted by the current cost and functionality of available commercial instruments. Although there are a number of low-cost turbidity sensors exploited within domestic ‘white-goods’, such as dishwashers, the lack of sensitivity, and power-usage of these devices make them unsuitable for fresh-water quality monitoring purposes. The recent introduction of wireless protocols and hardware, associated with the ‘Internet-of-Things’ concept for machine-to-machine autonomous sensing and control, has enabled the large-scale networked intelligent water turbidity monitoring system that implements relatively low-cost sensors to be developed. The proposed sensor uses both transmitted light and orthogonal (90 degrees) scattered light detection principles, and is 2–3 orders of magnitude lower in cost compared to the existing commercial turbidity sensors. With an 850-nm infrared LED, and dual orthogonal photodetectors, the proposed design is capable of measuring turbidity within the range of 0–1000 Nephelometric Turbidity Unit (NTU) with improved accuracy and robustness as compared with the existing low cost turbidity sensors. The combination of orthogonal and transmitted light detection unit provides both 0–200 NTU high resolution and accuracy sensing and 0–1000 NTU lower resolution and accuracy sensing capability. Results from calibration experiment are presented, which proved that the proposed sensor design produced comparable turbidity readings as that of a commercial turbidity sensor.

**Index Terms**—Turbidity measurement, turbidity sensors, fresh water quality, NTU, low cost, low power, Internet-of-Things (IoT), wireless.

## I. INTRODUCTION

**W**ATER quality monitoring plays a vitally important role in everyday life. Fresh-water quality management is heavily reliant on the instrumentation used. Parameters such as turbidity, colour, ambient temperature, etc. are often being utilised for this duty [1]. The level of suspended particulates within the aqueous stream, or bulk turbidity (‘haziness’), then provides a proxy measure for indicating an abnormal event, such as soil, residue and nutrients losses to the surrounding

water courses. Turbidity indicates the presence of suspended particulate matter (SPM) and other light-absorbing materials that affect the transmission of a light beam in the water body [2].

Traditionally turbidity measurements have involved on-site water sample collection and subsequent laboratory analysis, which is both labour-intensive and costly [3]. Several studies have shown that the need for continuous on-line water quality monitoring has become essential to the water industry and for ecosystem research [4], [5]. These studies have also proven the need for high spatial and temporal resolution of the on-line monitoring systems in order to recover adequate data on which to base downstream control measures or ecosystem models or both.

However, typically the cost and utility of commercial off the shelf (COTS) turbidity measurement products, such as those from Hach HST, the ‘GuardianBlue’ [6] or JMAR, the ‘BioSentry’ [7], which could satisfy the above requirements render them economically unviable for large scale adoption within water management and research. Moreover, the ease of implementation and deployment of such instruments are in most cases not ideal, requiring significant preparation before commissioning and post-project maintenance, including but not limited to works such as deployment site selection, infrastructure construction, periodical maintenance, etc.

Only recently, the concept of a low-cost turbidity sensing system has become achievable through the introduction of commodity devices, often two or three orders of magnitude cheaper than high-end products, which are typically used in ‘white-goods’, such as dishwashers.

The low-cost turbidity sensors mentioned above, which are currently available on the market, all use the same transmitted light detection principle, and are mainly applied in monitoring the haziness of water within dishwasher drainage lines. Unfortunately, due to their original intended use, these sensors do not have the capability of providing accurate and reliable turbidity sensing values for field deployments in rivers and water courses. From a sensor design perspective, as most of the turbidity readings in fresh-water systems will be within a range of 0–100 Nephelometric Turbidity Unit (NTU) [8], this would dictate an overall required range of 0–1000 NTU to track the extent of abnormal events, and with increased precision across a range of 0–100 NTU, which is aimed for detailed analysis of typical turbidity fluxes. The proposed sensor design complies with such requirements. Currently the sensor is configured to provide both 0–200 NTU and 0–1000 NTU measurements in consideration of tracking abnormal events using a combination

Manuscript received February 7, 2018; revised April 8, 2018; accepted April 9, 2018. Date of publication April 13, 2018; date of current version May 9, 2018. This work was supported by the University of Manchester, U.K. The associate editor coordinating the review of this paper and approving it for publication was Dr. Rosario Morello. (*Corresponding author: Bruce Grieve.*)

Y. Wang, S. M. S. M. Rajib, and B. Grieve are with the School of Electrical and Electronic Engineering, University of Manchester, Manchester M13 9PL, U.K. (e-mail: youchao.wang@student.manchester.ac.uk; smshariarmorshed.rajib@postgrad.manchester.ac.uk; bruce.grieve@manchester.ac.uk).

C. Collins is with the Environmental Science Research Division, Soil Research Centre, University of Reading, Reading RG6 6AB, U.K. (e-mail: c.d.collins@reading.ac.uk).

Digital Object Identifier 10.1109/JSEN.2018.2826778

of orthogonal (90 degrees) scattered and transmitted light detection units.

In addition, the rise of ‘Internet-of-Things’ (IoT) has provided the opportunities for this class of low-end turbidity sensors to be deployed for low-cost, networked monitoring. These sensors together with their platforms form what is known as the Wireless Sensor Network (WSN) where a group of spatially distributed sensor nodes monitor the physical conditions of the environment and transmit data to a central base. Through the development of sensors, WSNs that consist of a large number of sensor nodes, each being able to detect consistent physical sensing data, would be regarded as one of the key technologies for IoT [9]. Machine to machine (M2M) wireless communications, embedded within these WSNs allows autonomous connection and exchange of data between different nodes within the networks and real world [10].

Given the fact that there is a noticeable absence of low-cost turbidity sensor for large-scale continuous water quality monitoring deployment purpose, which is capable of providing 0-1000 NTU detection, meanwhile providing higher resolution within 0-200 NTU, as it being the sensor design consideration for this work, the originality in this work is in the design of a suitable turbidity sensor which is cheaper than the existing products, and is capable of delivering adequate specificity, sensitivity and reliability when incorporated into an integrated network of individual measurement nodes, i.e. an IoT sensor system. To achieve this, the design has focused on the reduction in the sensor power-budget, ease of implementation and the compatibility of its fit into various embedded platforms, suitable for large-scale IoT applications whilst minimising the overall system cost.

Although individually, each low-cost sensor unit may not have the accuracy to match the performance of the current high-end products, dynamic compensation for errors from any one node can be achieved by its deployment within an integrated network of similar sensors, enabling cross-correlation of the values obtained following suitable correction for temporal variations and building on historical calibration records for all or a subset of the sensors.

The proposed self-designed sensor is capable of providing reliable turbidity values within the range of 0-200 NTU with 0.1 NTU level precision, whilst also having the ability to detect and track values up to 1000 NTU with a lower precision and accuracy. The design offers ease-of-implementation within the host IoT device or platform, requiring only four connections, comprised of a constant 5V power supply, 0V ground and dual sensor output lines.

The remaining of this paper is organized as follows. Section II reviews related work. Section III presents the design principle and measurement method, as well as the structural overview of the sensor design. Section IV briefly discusses the lab experiment setup followed by the illustration of lab results and further discussions in Section V. Finally, the paper is concluded in Section VI.

## II. RELATED WORK

It is surprising that although turbidity measurement and monitoring have long been a research focus, only several

attempts have been made into designing and implementing low-cost sensors for fresh-water quality management purposes. The majority of water quality monitoring products, as stated in the preceding section, and turbidity sensor designs [11], [12] are sophisticated and often costly, which therefore does not meet the overall aim of this work.

A variety of WSN enabled on-line water quality monitoring systems have been proposed using either COTS sensors [13]–[15] or self-designed sensors [16], [17] to monitor the water quality changes within domestic running water, lakes and rivers. These WSN systems are typically low in power consumption and rely heavily on the sensors and instruments implemented within the platforms. However, none of the systems listed above, implementing low-cost COTS sensors proved the capability of delivering turbidity values from 0 to 1000 NTU with adequate precision and accuracy.

Authors in Azman *et al.* [16] proposed a sensor design using nephelometric method for the system, a photodetector placed 90 degrees from the light source detects the scattered light intensity. A microcontroller controls the LED light source and the orthogonal light detection receiver. A calibration experiment was carried out to test the performance of the fabricated sensor. Although the sensor was proved to be reliable for water quality monitoring purpose, the results did not point out the sensor’s capability of measuring samples above 100 NTU.

A low cost sensor design which utilizes ratio method for on-line monitoring has been developed by Lambrou *et al.* [17]. This design is identical to the COTS low-cost products, which initially utilizes transmitted light detection. In the design, an improvement of adding an orthogonal detection unit was made in order to improve its accuracy. By calibration, the designed sensor is capable of providing 0.1 NTU level precision with ideal accuracy. However, the authors did not further provide details on how the  $\pm 0.5$  NTU accuracy of the demonstrated sensor was obtained, and the detection range was limited to only 0-100 NTU.

## III. DESIGN OF SENSOR

### A. Design Principle and Measurement Method

Considering the need for higher precision and accuracy within the detection range of 0-100 NTU, a more sophisticated design approach, as compared to using a simpler transmitted light detection design, to measure the NTU [2] is applied for the design and follows ISO7027 Standard [18].

According to ISO7027 Standard [18], a light source should be near-infrared with a wavelength of  $860 \pm 30$ nm in order to minimize the interference caused by coloured samples that are light-absorbing.

Due to the availability of the light source, a near-infrared 850nm LED (VSLY 5850, Vishay Electronic GmbH, Selb, Germany) was chosen as the constant source of light. A 5V dc power supply and a series 470-ohm resistor were used to provide a constant LED supply current.

The primary NTU measurements are taken using a photo-transistor, positioned orthogonally with respect to the direction of the original light, to detect the intensity of light which is scattered at 90 degrees to the original light beam. The scattered

light intensity is proportional to the actual turbidity [19],

$$T = k_1 I_{90} + k_2, \quad (1)$$

where  $T$  is the turbidity of waterbody, and  $I_{90}$  is the intensity of the nephelometric scattered light detected at 90 degrees. Both the parameters  $k_1$  and  $k_2$  are chosen during the calibration.

The primary measurement unit will only be targeting at 0-200 NTU, so that the per NTU output voltage difference could be maximized. In order to provide an overall 0-1000 NTU detection capability, another light detection unit which detects the transmitted light intensity was also implemented in order to provide a full precision range. The photodiode used for transmitted light detection is positioned in-line the light path. The relationship between the detected light intensity and actual turbidity is exponential [20], thus

$$I_{trans} = k_3 e^{-\frac{1}{k_4} T}, \quad (2)$$

where  $I_{trans}$  is the transmitted light intensity detected by the sensor,  $T$  denotes the turbidity of waterbody, and  $k_3$  and  $k_4$  are parameters determined during the sensor calibration stage. The turbidity  $T$  is therefore given by

$$T = -k_4 (\ln I_{trans} - \ln k_3). \quad (3)$$

For a fixed spectrum of light, 850 nm in this case, due to the availability of the light source diode, photodetectors being used for light detection would output currents that are directly proportional to the intensity of light being detected. These currents are then transferred to voltage outputs using op-amps and resistors with fixed values. Therefore, the equations could be further denoted as,

$$T = \beta_1 \times V_{90} + \beta_2, \quad (4)$$

$$T = -\beta_4 (\ln V_{trans} - \beta_3), \quad (5)$$

where  $T$  denotes the turbidity of waterbody,  $V_{90}$  and  $V_{trans}$  are the voltage outputs of the 90 degrees light detection unit and the transmitted light detection unit respectively. The parameters  $\beta_1, \beta_2, \beta_3, \beta_4$  are determined during the calibration.

Theoretically, even when the base of the NPN phototransistor is not connected and wired, the light sensitivity of a phototransistor still outperform a photodiode by providing an additional gain in the case of low light detection [21]. Therefore, using phototransistor as primary device becomes the preferred choice for low intensity light detection in low turbidity situations.

However, it is still of the same importance to take power budget and accuracy into consideration. A phototransistor (BPW77NB, Vishay Electronic GmbH, Selb, Germany) was chosen despite the power constraints due to the necessary amplification of the received light signal. Typically, phototransistors output current that is orders of magnitude larger than that from photodiodes. In terms of power budgeting, photodiodes tend to be less power consuming.

As a result, the present design uses the BPW77NB for orthogonal scattered light detection, and a photodiode (BPW24R, Vishay Electronic GmbH, Selb, Germany) for transmitted light detection.

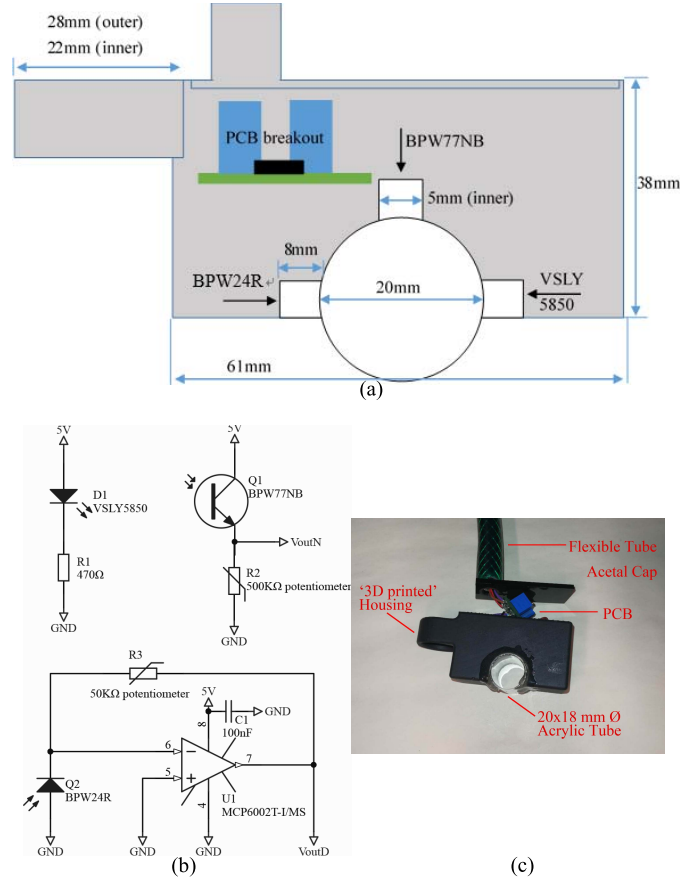


Fig. 1. (a) Dimensional layout of hardware. The 20mm diameter hole is used for acrylic tube adhesion, water flows through the tube during measurements. (b) Circuit schematic design. Four pin connections are required, 5V, 0V ground and dual sensor output pins ( $V_{outN}$  and  $V_{outD}$ ). (c) Overall structural view of the sensor.

## B. Structural Design Overview

The structure dimensions and components layout are shown in Fig. 1. An extruded transparent Acrylic tube of the size 20mm (outer diameter)  $\times$  18mm (inner diameter) is adhered onto the 3D-printed housing as pointed out in Fig. 1 (a), in order to provide a channel for the turbidity fluxes to pass through. Waterproof transparent epoxy is used for adhesion. The analogue circuitry is presented in Fig. 1 (b), and the overall structural view of the sensor is presented in Fig. 1 (c).

The sensor housing is currently 3D-printed using stereolithography (Form2 3D printer, Formlabs Inc., Somerville, USA) with black resin to minimize the colour effects, with considerations such as ease of fabrication and capability of providing water-tightness. Although the total cost of the sensor is currently higher than the off-the-shelf products, which is due to the requirement of 3D-printed housing and the Printed Circuit Board (PCB) production, it is believed that a mass bespoke production could further decrease the overall cost in the future through mass production techniques, such as injection moulding of the case and automated surface mounting of PCB components. By further minimizing the area and volume of the PCB and sensor housing respectively, the cost for such

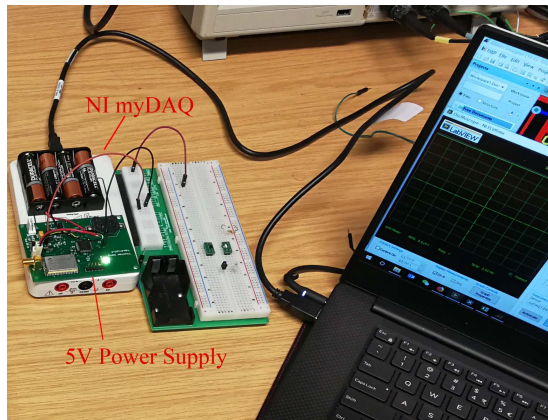


Fig. 2. Calibration experiment setup. 5V power and 0V ground were supported by a customized hardware platform using 4 x AA batteries. NI myDAQ was used for data-logging.

productions can be minimized and controlled to within an acceptable range.

Generally, this sensor design maintains the low-cost property, as compared to the high-end products that are of two to three orders of magnitude higher in cost.

#### IV. LAB EXPERIMENT SETUP

An indirect method to calibrate the sensor and further examine the performance was carried out during the calibration process, avoiding the use of expensive NTU standard solutions. A HI 93703 turbidity measuring instrument (HANNA Instruments Inc., Rhode Island, USA), which is capable of measuring the turbidity values ranging from 0 to 1000 NTU, providing  $\pm 0.5$  NTU or  $\pm 5\%$  of reading accuracy, whichever is greater [22], was used to provide reference turbidity values.

The required 5V constant dc power supply for the sensor was supported by a customized IoT platform which utilizes four 1.5V 2700mAh industrial Alkaline batteries as shown in Fig. 2. As a convenient interface for data-analysis [23], a ‘myDAQ’ general purpose interface unit (National Instruments Corporation, Austin, USA) was used to log the sensors’ voltage outputs into computer for further data-processing. The actual turbidity of each solution sample is measured using HI 93703 at the same time when measuring the voltage outputs of sensors to minimize the error caused by the change of turbidity within the water samples. An emulsion concentrate of fat particulates within an aqueous continuous phase was added to distilled water in order to adjust the turbidity and undertake sensor calibration. The turbidity values of each water sample shown in Fig. 3 were chosen to be representative across the anticipated operating range of the device.

The potentiometers on the PCB breakout board translated the currents from the two photo-devices into voltage outputs. Then the voltage values were read and captured by the myDAQ oscilloscope, and logged into computer for further data analysis.

In total five sets of orthogonal detection units and six sets of transmitted light detection units were calibrated and tested separately, the values of the on-board potentiometers were adjusted so that the general performance of each set of



Fig. 3. Prepared solution as water samples, the concentration of fat particulates within each sample was changed by mixing the particles with distilled water. HI 93703, as a reference meter, was used to determine the turbidity of each sample.

sensors is identical. All sensors were adjusted so that each orthogonal detection unit outputs circa 1.9V in a 100 NTU sample and approximately 4.5V in a 250 NTU sample, and each transmitted detection unit outputs 4.5V in a 0 NTU sample to maximize the output voltage range.

The potential effects on the sensor from diurnal variations in ambient environmental conditions were investigated through dividing the test set of 5 sensor systems into two groups which were then analysed under typical humidity and temperature conditions found at a fixed time points during the day, at 12:00 and 20:00.

To further examine the linearity region of the transmitted light detection unit, another set of sensors (set 6) were tested in the same environment, with 10 samples across a range of turbidity concentrations distributed over a range from 0 to 947 NTU.

All the voltage output values in different water samples were captured 5 times per acquisition cycle and an average value was then calculated to minimize the errors caused by noise. Sample values above 1000 NTU were not tested due to the range limitations of reference HI 93703 instrument and the overall design requirements.

#### V. RESULTS AND DISCUSSION

##### A. Improved Sensitivity and Accuracy

As may be seen from the Fig. 4 and Fig. 5, the sensor exhibits output patterns with an appropriate degree of linearity. The R-squared values which indicate the goodness to fit, to two decimal places of precision, when finding the best-fit straight line for each set of sensors, are as high as 99.81% for the orthogonal light detection unit, and 99.36% for the transmitted light detection unit. Consequently, the sensor is capable of providing 0.01V resolution per turbidity unit (NTU) in low turbidity samples which, from the data acquisition perspective, offers the potential to deliver 0.1 NTU accuracy if each unit is individually calibrated.

From Fig. 4, it may be concluded that for samples from approximately 270 NTU and onwards, the primary orthogonal

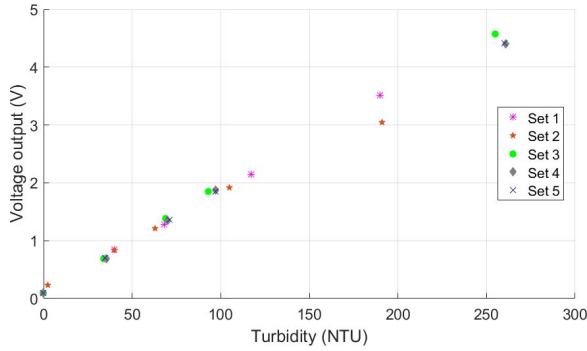


Fig. 4. The voltage outputs for orthogonal detection unit in different water samples.

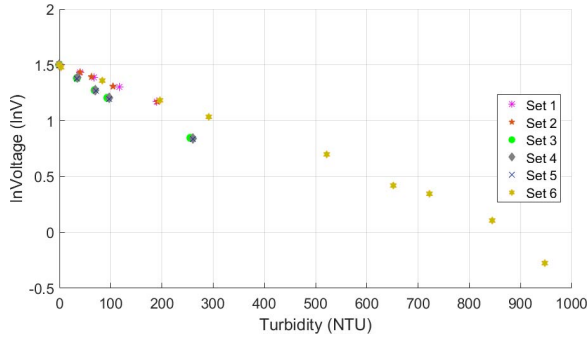


Fig. 5. The voltage outputs (logarithmic scale) of transmitted detection units in different water samples.

light detection unit would lose its linearity due to the limited voltage input/output range of the platform device. At this point, the transmitted light detection unit is then configured to become the primary source of the measurement, which could ultimately provide sensed turbidity values to over 1000 NTU.

The first two sets of sensors were calibrated using five water samples with ascending turbidity values to prove that the sensors provide linearity within the proposed 0-200 NTU region, while the remaining sets of sensors used samples above 250 NTU to exploit the maximum region of linearity based on current settings.

By comparing different sets of sensors' behaviour in Fig. 5, sets 1, 2 and 6 are identical with each other while sets 3, 4 and 5 output roughly the same results. As pointed out previously, only set 6 was tested in its full range of 0-1000 NTU, while the other five sets were calibrated for the 0-200 NTU range. Given the use of same sensor technique, a reasonable assumption has been made that the 0-1000 NTU calibration curve for one of the units could be used to extrapolate a similar range for the remainders.

Table I and Table II show the calibration configurations for each separate set of sensors, as well as the fit to a linear calibration line, which indicates the appropriate degree of linearity, note that the linearity of transmitted light sensing is in log-scale. The best-fit straight lines for orthogonal detection units exhibit less error between true values and the fitted values as compared to those in transmitted detection units. Although for both cases errors, which could be as high as 8% (orthogonal) and 15% (transmitted) respectively, may be found in different calibration curves, the general trends are

TABLE I  
THE RESISTANCE SETUP AND CALIBRATION CURVES  
FOR THE TESTED SENSORS

Sensor model	Resistance (90 deg)	$T = \beta_1 \times V_{90} + \beta_2(R^2)$
Set 1	330K $\Omega$	$T = 55.984x - 5.4317(0.999)$
Set 2	290K $\Omega$	$T = 66.508x - 16.085(0.997)$
Set 3	390K $\Omega$	$T = 57.015x - 8.0085(0.999)$
Set 4	390K $\Omega$	$T = 60.656x - 9.4765(0.998)$
Set 5	330K $\Omega$	$T = 60.444x - 9.2644(0.999)$

TABLE II  
THE RESISTANCE SETUP AND CALIBRATION CURVES  
FOR THE TESTED SENSORS

Sensor model	Resistance (trans)	$T = -\beta_4(\ln V_{trans} - \beta_3)(R^2)$
Set 1	43.2K $\Omega$	$T = -570.10 \ln V_{trans} + 858.55(0.9997)$
Set 2	26.1K $\Omega$	$T = -582.82 \ln V_{trans} + 873.04(0.998)$
Set 3	21.4K $\Omega$	$T = -393.25 \ln V_{trans} + 578.84(0.988)$
Set 4	35.3K $\Omega$	$T = -400.22 \ln V_{trans} + 589.78(0.990)$
Set 5	21.9K $\Omega$	$T = -399.82 \ln V_{trans} + 586.14(0.991)$
Set 6	21.1K $\Omega$	$T = -566.18 \ln V_{trans} + 873.12(0.986)$

identical between different modules that have individually adjusted resistances.

It is concluded from Table III - V that the difference in turbidity reading between the orthogonal detection unit and the commercial turbidity meter, HI 93703, is less than 10%, and the difference between transmitted light detection unit and the turbidity meter circa 20%, suggesting lower accuracy as compared to the orthogonal case. This significant difference in the readings provided by the transmitted light detector and reference turbidity meter's output, is due to the former being configured for lower precision, in order to achieve a wider detection range. Unfortunately, as shown in Table V, the wide-range configuration has led to unacceptable errors in low turbidity cases, in contrast such a behaviour was not found in the cases shown in Table IV when the transmitted unit was calibrated using a low turbidity (0-200 NTU) calibration curve. Hence, a software side value offsetting would be necessary if samples below 100 NTU are to be measured by the transmitted light detection unit. This is mainly because the applied curve fitting offsets the turbidity values by approximately 20 NTU in low turbidity cases.

In order to carry out accurate turbidity measurements, it is proposed that the orthogonal detection unit should only be used for 0 to 200 NTU detection. Operationally, this means that the orthogonal detector may be configured to turn on when the detection cycle is initiated and the signals from it are then only recorded when the turbidity of the sampled water/solution falls within the range of 0 to 200 NTU, so to achieve the highest accuracy and lowest power consumption for the

TABLE III  
THE COMPARISON BETWEEN DESIGNED SENSOR SET 3  
AND TURBIDITY METER

Sample	Turbidity	Turbidity (90 deg)	Turbidity (90 deg) in NTU	% NTU relative error (difference)
1	0.00NTU	0.205V	-2.12NTU	N/A
2	34.01NTU	0.694V	31.53NTU	7.29%
3	69NTU	1.387V	71.13NTU	-3.09%
4	93NTU	1.854V	97.82NTU	-5.18%
5	255NTU	4.576V	253.36NTU	0.64%

TABLE IV  
THE COMPARISON BETWEEN DESIGNED SENSOR SET 1  
AND TURBIDITY METER

Sample	Turbidity	Turbidity (trans)	Turbidity (trans) in NTU	% NTU relative error (difference)
1	0NTU	4.50V	0.51NTU	N/A
2	39.8NTU	4.20V	40.75NTU	2.39%
3	68NTU	4.01V	66.99NTU	-1.49%
4	117NTU	3.68V	115.50NTU	-1.28%
5	190NTU	3.22V	191.06NTU	0.58%

whole sensor system. The lower accuracy, but wider range transmitted light detection unit would then be energised at all times for monitoring the water course turbidity levels, and switching-in the orthogonal light detector when appropriate, as well as for cross-correlation purposes, with the orthogonal detector.

### B. Repeatability and Consistency

It should be noted that each separate sensor would be required to perform calibration individually, in order to obtain their optimum performance. Within this investigation, five sets of sensors, with the same layout and structure, were tested for consistency. The results shown in Fig. 4 and Fig. 5 reveal the limitations and errors that exist due to the constraints imposed by the current working process. The light detection unit's performance could be affected by not only the transparency of the tube selected, but also the errors within PCB boards, photodetectors and resistors. Inevitably, individual calibration will be required when setting up the sensors, so that the systematic errors caused by fabrication process and individual device characteristic variations could be correlated and minimized.

By comparing the calibration curve fitting results and the potentiometer settings between different sets of sensors, it may be found that the sensors behave identically, and the overall design is capable of providing crosscheck consistency and reliability for mass production, as long as the sensors are calibrated individually. The sensors investigated exhibited identical relative behaviours, although individual differences

TABLE V  
THE COMPARISON BETWEEN DESIGNED SENSOR SET 6  
AND TURBIDITY METER

Sample	Turbidity	Turbidity (trans)	Turbidity (trans) in NTU	% NTU relative error (difference)
1	0NTU	4.50V	21.54NTU	N/A
2	3.28NTU	4.40V	34.27NTU	944%
3	83NTU	3.89V	104.02NTU	25.32%
4	196NTU	3.26V	204.05NTU	4.11%
5	292NTU	2.82V	286.54NTU	-1.87%
6	522NTU	2.01V	478.13NTU	-8.40%
7	652NTU	1.52V	636.80NTU	-2.33%
8	722NTU	1.41V	676.98NTU	-6.24%
9	845NTU	1.11V	813.01NTU	-3.79%
10	947NTU	0.76V	1028.50NTU	8.61%

and errors between them exist, due to factors such as specific variations in photodetectors, and other sensitive components due to inconsistency within their fabrication.

### C. Temperature Correlation

The existing relationship between ambient temperature and accuracy of turbidity sensing requires the temperature corrections to take place during the system's data-processing stage. Errors caused by the change of relative collector currents of the photo-devices under different ambient temperature conditions should ideally be compensated for. In the extreme cases, such as where the temperature difference between summer and winter or day and night differs greatly, with 30 degrees Celsius of transitions, e.g. from 0 degrees Celsius to 30 degrees Celsius, the output current would differ by a factor of 1% [24] and 40% [25] respectively considering the implementation of both photodiode and phototransistor. Moreover, the radiant power and peak wavelength of LED are also subject to change with the fluctuation of temperature [26], which would cause the change of the output light, and consequently affecting the obtained results.

In addition, the relative changes of the resistors' physical property, which are associated with the temperature drift, should also be taken into consideration. Therefore, a reliable low-cost temperature sensor needs to be implemented so that the influence caused by the change of ambient temperature in waterbody could be eliminated. Care should be taken regarding the change of ambient water temperature, and hence research into temperature correlation for low-cost turbidity sensor design is expected to be regarded as an important design aspect.

## VI. CONCLUSION & DISCUSSION

The paper has reported on the delivery of a generic turbidity sensor design and validation that it indicates that it is possible to lower the current cost of deploying turbidity-monitoring

units, for fresh-water quality monitoring by a significant factor. The latter design has focused on a specific manifestation of that sensor that is both compatible with IoT networks, in terms of unit cost, power-usage, reliability, size, etc., as well as reliant on being incorporated as part of such a network.

The unit has been designed to provide acceptable relative precision and response times such that the absolute precision may be enhanced through the analysis of the temporal modelling of the fluxes in the individually sensed real-time turbidity measurements, across the network, versus specific points in time and space where absolute reference measures of turbidity are obtained and/or known turbidity events occurred, due to analysis of the associated meta-data, e.g. flood events, specific field applications, etc.

Consequently, the sensor is capable of providing high accuracy output (10% difference comparing to the high accuracy reference instrument HI 93703) with 0.1 NTU precision within the range of 0-200 NTU and a lower-accuracy (20% difference) of 1.0 NTU precision output for 0-1000 NTU. The current Bill-of-Materials is 2-3 orders of magnitude lower than the non-IoT compliant existing technology, with the potential for further value-engineering to lower the cost by at least another order of magnitude.

In order to minimize labour cost, which is added due to the currently required calibration procedure, future work would also look into the possibilities of adding self-calibration and auto-calibration capabilities for the sensor. From the experiment, it is found that different sets of sensor's behaviour are identical, hence it becomes possible by applying machine-learning algorithm to cross-correlate with other sensors *in situ* to auto-calibrate individually once these sensors were deployed in the same region. It is expected that, as long as the sensor is not coated/fouled to an undetectable extent, the two light detection units could always function as a cross-correlation pair, and provide useful measurement data to minimize the coating effect by exploiting *in situ* calibration capability.

The work to-date has shown that a turbidity sensor, which combines orthogonal (90 degrees) light detection and transmitted light detection unit in a way that could provide both 0-200 NTU and 0-1000 NTU measurements with comparatively modest precision between calibrations, and is suitable for wireless monitoring duties, can be designed and fabricated within a cost-effective, low-power and miniature package. In achieving the latter, the system is now available and has been deployed in 2017 within field units in the UK, to enable bulk suspended particulates to be monitored in real-time along an exemplar water course in the Southeast of England. From the sensor design perspective, research into individual self-calibration functionality and cross-calibration against neighbours and mega data will be one of the possible approaches to further improve overall accuracy of low-cost turbidity sensors.

This research opens up the possibility for optimised reference sampling and analysis of compositional perturbations in and around water courses irrespective of geography. As an exemplar scenario, remotely located IoT sensors, as proposed, in most cases, must operate with a limited duty cycle, i.e. minimising battery usage versus trickle charge from power harvesting, such as photovoltaics. The proposed sensor offers

the opportunity to both 'wake-up' and increase the sampling rate for downstream IoT sensors, so that the detailed geographic and temporal spread of a flux in the measurement values may be mapped as well as retrospective cross-correlation of that high 'granularity' data versus spot laboratory reference samples. With the potential for dynamic control of the network, the 'shape' of the turbidity flux of an event within a water course, as identified by one or more upstream IoT devices, could then be analysed to control, in real-time both the sampling frequency of the subsequent IoT sensors within the system and the optimum point at which to extract a representative water aliquot, for reference laboratory analysis of the event.

In addition, this research has shown that the range of sensors currently utilised on a significant scale, but in small numbers, by the water and environmental management community are also applicable to fundamental re-engineering into an IoT compatible reduced format, that can then accept sensor modalities that may have been rejected as being too expensive or lacking specificity in the past, e.g. Dissolved Oxygen, Electrical Impedance, Potentiometric sensing, Near-Near Infra-Red / Visible / Ultraviolet (fluorescence) spectroscopy.

#### ACKNOWLEDGMENT

The authors would like to thank the reviewers for their valuable inputs and suggestions to improve the quality of this paper.

#### REFERENCES

- [1] D. Chapman, *Water Quality Assessments: A Guide to the Use of Biota, Sediments and Water in Environmental Monitoring*, vol. 2. Cambridge, U.K.: Cambridge Univ. Press, 1996, p. 609.
- [2] J. Downing, "Turbidity monitoring," in *Environmental Instrumentation and Analysis Handbook*. Hoboken, NJ, USA: Wiley, 2005, pp. 511–546.
- [3] O. Korostynska, A. Mason, and A. I. Al-shamma, "Monitoring pollutants in wastewater: Traditional lab based versus modern real-time approaches," in *Smart Sensors for Real-Time Water Quality Monitoring*, vol. 4, S. C. Mukhopadhyay and A. Mason, Eds. Berlin, Germany: Springer-Verlag, 2013, pp. 1–24. [Online]. Available: [https://www.springer.com/gb/book/9783642370052?wt\\_mc=ThirdParty\\_SpringerLink.3.EPR653.About\\_eBook#otherversion=9783642370069](https://www.springer.com/gb/book/9783642370052?wt_mc=ThirdParty_SpringerLink.3.EPR653.About_eBook#otherversion=9783642370069), doi: 10.1007/978-3-642-37006-9.
- [4] J. Bhardwaj and K. K. Gupta, "A review of emerging trends on water quality measurement sensors," in *Proc. Int. Conf. Technol. Sustain. Develop. (ICTSD)*, 2015, pp. 1–6.
- [5] S. Panguluri, G. Meiners, J. Hall, and J. G. Szabo, "Distribution system water quality monitoring: Sensor technology evaluation methodology and results," Environ. Protection Agency, Washington, DC, USA, Tech. Rep. EPA 600/R-09/076, Oct. 2009, pp. 1–60. [Online]. Available: [https://cfpub.epa.gov/si/si\\_public\\_record\\_report.cfm?dirEntryId=212368](https://cfpub.epa.gov/si/si_public_record_report.cfm?dirEntryId=212368)
- [6] HACH Company. (2017). *GuardianBlue Early Warning System*. Accessed: Dec. 1, 2017. [Online]. Available: <https://www.hach.com/event-detection-and-security/guardianblue-early-warning-system/family?productCategoryId=3554762778>
- [7] JMAR Advanced Technologies. *BioSentry Monitoring System for Water-born Microorganisms*. Accessed: Nov. 30, 2017. [http://www.interline.nl/media/1000116/biosentry\\_wms\\_v3.2.pdf](http://www.interline.nl/media/1000116/biosentry_wms_v3.2.pdf)
- [8] Environment Agency, Bristol, U.K. (2017). *Water Quality Data Archive*. Accessed: Nov. 30, 2017. [Online]. Available: <http://environment.data.gov.uk/water-quality/view/landing>
- [9] S. Yinbiao *et al.*, "Internet of Things: Wireless sensor networks," Int. Electron. Commission, Geneva, Switzerland, White Paper IEC WP IoT:WSN:2014-11(en), 2014, pp. 1–78.
- [10] T. Fan and Y. Chen, "A scheme of data management in the Internet of things," in *Proc. 2nd IEEE Int. Conf. Netw. Infrastruct. Digit. Content*, Sep. 2010, pp. 110–114.

- [11] X. Dai, S. J. Sheard, D. O'Brien, S. Russell, and L. Carswell, "Propagation and scattering model of infrared and ultraviolet light in turbid water," in *Proc. 22nd Wireless Opt. Commun. Conf. (WOCC)*, May 2013, pp. 601–606.
- [12] C.-T. Chiang, S.-M. Huang, and C.-N. Wu, "Development of a calibrated transducer CMOS circuit for water turbidity monitoring," *IEEE Sensors J.*, vol. 16, no. 11, pp. 4478–4483, Jun. 2016.
- [13] V. Raut and S. Shelke, "Wireless acquisition system for water quality monitoring," in *Proc. Conf. Adv. Signal Process. (CASP)*, 2016, pp. 371–374.
- [14] R. Yue and T. Ying, "A water quality monitoring system based on wireless sensor network & solar power supply," in *Proc. IEEE Int. Conf. Cyber Technol. Autom., Control, Intell. Syst.*, Mar. 2011, pp. 126–129.
- [15] F. Adamo, F. Attivissimo, C. G. C. Carducci, and A. M. L. Lanzolla, "A smart sensor network for sea water quality monitoring," *IEEE Sensors J.*, vol. 15, no. 5, pp. 2514–2522, May 2015.
- [16] A. A. Azman *et al.*, "A low cost nephelometric turbidity sensor for continual domestic water quality monitoring system," in *Proc. IEEE Int. Conf. Autom. Control Intell. Syst. (I2CACIS)*, Oct. 2016, pp. 202–207.
- [17] T. P. Lambrou, C. C. Anastasiou, C. G. Panayiotou, and M. M. Polycarpou, "A low-cost sensor network for real-time monitoring and contamination detection in drinking water distribution systems," *IEEE Sensors J.*, vol. 14, no. 8, pp. 2765–2772, Aug. 2014.
- [18] *Water Quality—Determination of Turbidity*, ISO Standard 7027, 2016.
- [19] C. C. Hach and M. Sadar, *Turbidity Standards: Technical Information Series Booklet No. 12*. Loveland, CO, USA: Hach Company, 1985.
- [20] H. Liu *et al.*, "Generalized weighted ratio method for accurate turbidity measurement over a wide range," *Opt. Exp.*, vol. 23, no. 25, pp. 32703–32717, 2015.
- [21] P. Kostov, W. Gaberl, M. Hofbauer, and H. Zimmermann, "PNP PIN bipolar phototransistors for high-speed applications built in a 180 nm CMOS process," *Solid-State Electron.*, vol. 74, no. 5, pp. 49–57, 2012.
- [22] *Instruction Manual HI 93703*, HANNA Instrum., Woonsocket, RI, USA, 2005.
- [23] National Instruments Corporation. (2017). *What Is myDAQ—Product Page*. Accessed: Dec. 3, 2017. [Online]. Available: <http://www.ni.com/en-gb/shop/engineering-education/portable-student-devices/mydaq/what-is-mydaq.html>
- [24] *Silicon PIN Photodiode, RoHS Compliant 948642, BPW24R Datasheet*, Vishay Semicond., Malvern, PA, USA, 2011.
- [25] *Silicon NPN Phototransistor, RoHS Compliant 94, BPW77NB Datasheet*, Vishay Semicond., Malvern, PA, USA, 2008.
- [26] *High Speed Infrared Emitting Diode, 850 nm, Surface Emitter Technology, VSLEY850 Datasheet*, Vishay Semicond., Malvern, PA, USA, 2013.



**Youchao Wang** is currently pursuing the B.Eng. degree in electronic engineering from the University of Manchester (UoM), Manchester, U.K. He is under a joint degree program, and will eventually receive the B.Eng. (Hons.) degree in electronic engineering from UoM, and the B.Eng. degree in electrical and electronic engineering from North China Electric Power University, Beijing, China, in 2018. His research interests include wireless sensor networks, Internet of Things applications, and optical sensor design.



**S. M. Shariar Morshed Rajib** received the M.Eng. degree in electrical and electronic engineering from the University of Manchester, Manchester, U.K., in 2017, where he is currently pursuing the Ph.D. degree in electrical and electronic engineering, researching on the potential of Internet of Things-based devices in agriculture. His current research interest includes wireless sensor networks, embedded systems, and data analysis.



**Chris Collins** is the Chair of Environmental Chemistry at the University of Reading. He is the Natural Environment Research Council Soils Coordinator overseeing a £10 M research investment to improve our understanding of how soils resist, recover and adapt to land use, and climate change. His research interests include determining the factors controlling exposure of biota to environmental pollution. This combines experimental data with process description models and developing assessment tools to assess the bioaccessibility of pollutants in the human gut, and model systems to determine uptake of soil contaminants by plants and earthworms. Prof. Collins chairs the Department for Environment, Food and Rural Affairs Hazardous Substances Advisory Committee providing expert advice to the U.K. Government on how to protect the environment, and human health via the environment from chemicals. This paper has been supported by a wide range of funders across industry, government, and research bodies.



**Bruce Grieve** is a Fellow of the Institute of Engineering and Technology, the Institute of Agricultural Engineers, and the Higher Education Academy. He holds the N8 Chair at Agri-Sensors and Electronics. Before joining the University of Manchester, as the Director of the e-Agri Sensors Centre, he gained 18 years of industrial experience in the fields of online analysis and measurement research and development, including deployment of sensors and informatics systems within new integrated products for sustainable agriculture and food. Since 2007, he has attracted over £5.3 M of direct industrial, governmental, and NGO funding which has been leveraged against a portfolio of £20.4 M in collaborative multidisciplinary research projects. Prof. Grieve has been the Industrial Manager on a number of U.K. Research Council and DTI supported projects. He received the Royal Academy of Engineering Senior Fellowship to progress his e-Agri research at the University of Manchester. He has held a number of funding board roles with the U.K. Research Councils and the Innovate-UK (TSB), including being a nominated member of the BBSRC Agriculture and Food Security Strategy and Policy Panel and the STFC 21st Century Challenges Strategy Panel.